DE GRUYTER OPEN

Acta Geophysica
vol. 63, no. 1, Feb. 2015, pp. 1-16
DOI: 10.2478/s11600-014-0227-4

The 2014 Kefalonia Doublet (M_w6.1 and M_w6.0), Central Ionian Islands, Greece: Seismotectonic Implications along the Kefalonia Transform Fault Zone

Vassilios KARAKOSTAS, Eleftheria PAPADIMITRIOU, Maria MESIMERI, Charikleia GKARLAOUNI, and Parthena PARADISOPOULOU

Geophysics Department, Aristotle University of Thessaloniki, Thessaloniki, Greece
e-mails: vkarak@geo.auth.gr, ritsa@geo.auth.gr (corresponding author), mmesimer@geo.auth.gr, hagarl@geo.auth.gr, ppara@geo.auth.gr

Abstract

The 2014 Kefalonia earthquake sequence started on 26 January with the first main shock (M_w 6.1) and aftershock activity extending over 35 km, much longer than expected from the causative fault segment. The second main shock (M_w 6.0) occurred on 3 February on an adjacent fault segment, where the aftershock distribution was remarkably sparse, evidently encouraged by stress transfer of the first main shock. The aftershocks from the regional catalog were relocated using a 7-layer velocity model and station residuals, and their distribution evidenced two adjacent fault segments striking almost N-S and dipping to the east, in full agreement with the centroid moment tensor solutions, constituting segments of the Kefalonia Transform Fault (KTF). The KTF is bounded to the north by oblique parallel smaller fault segments, linking KTF with its northward continuation, the Lefkada Fault.

Key words: 2014 Kefalonia earthquake, Kefalonia Transform Fault, aftershocks, step-over zone, seismotectonics.

1. INTRODUCTION

On 26 January 2014 an M_w 6.1 earthquake occurred in the western part of Kefalonia Island, the most seismically active region in the Aegean and surrounding areas (Fig. 1). The activated area is part of the Kefalonia Transform Fault Zone (KTFZ), ~100 km long, consisting of the Kefalonia and Lefkada Fault branches, and linking the continental collision with the oceanic subduction zones, in the Ionian Sea (Greece). Scordilis *et al*. (1985) first suggested that the 1983 Kefalonia earthquake (M7.0) had a dextral strike-slip mechanism. The mainly strike-slip motion of the Kefalonia Fault was confirmed by waveform modeling for the 1983 earthquake by Kiratzi and Langston (1991) and for the 17 September 1972 earthquake (M6.3) by

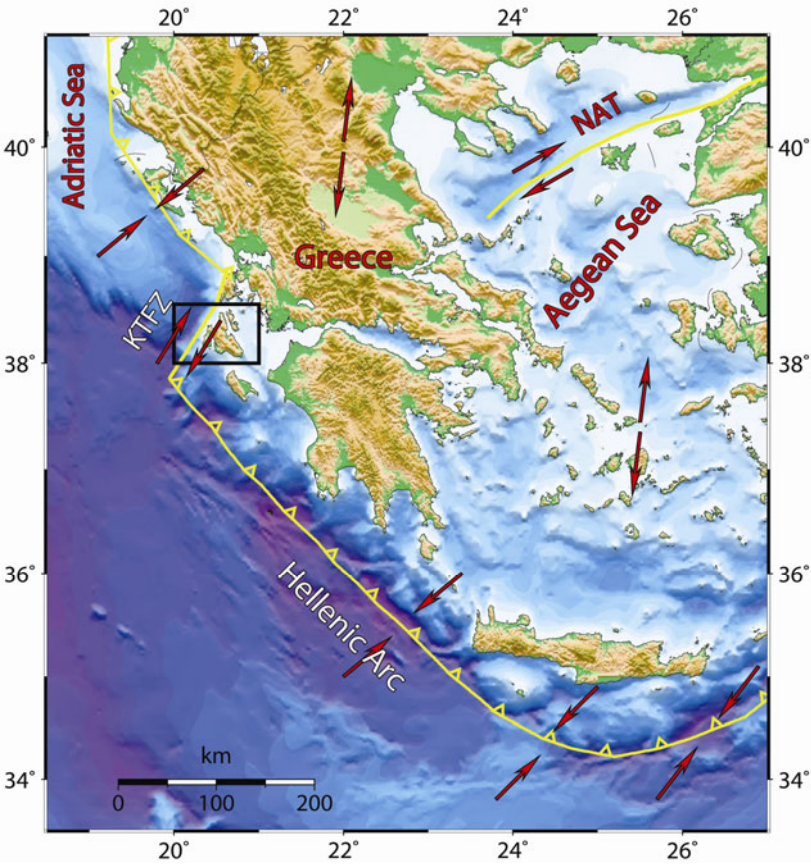

Fig. 1. The main geodynamic features of the Aegean and surrounding areas shown on a relief map. The active boundaries are shown as solid lines. The arrows indicate the approximate direction of relative plate motion. The study area is denoted by the square. KTFZ – Kefalonia Transform Fault Zone, NAT – North Aegean Trough.

Papadimitriou (1993). Later on, Louvari *et al*. (1999) investigated the strike slip nature of both Kefalonia and the adjacent Lefkada Fault branches, with maximum reported earthquake magnitudes of 7.4 and 6.6, respectively (Papazachos and Papazachou 2003). The fault zone follows the submarine Kefalonia valley, west of the island chain from Lefkada to Kefalonia. The southern prolongation of the KTFZ was shown by seismic line data and fault plane solutions located south of Kefalonia in the Ionian abyssal plain (Kokinou *et al*. 2006). For this region complete historical information exists for strong ($M \geq 6.5$) earthquakes in the last five centuries, revealing an average of about one such shock per decade (Papadimitriou and Papazachos 1985). These events have repeatedly destroyed urban areas, producing extensive damage and loss of life, with the most severe one being the 1953 paroxysm with four events (9 August, $M6.4$; 11 August, $M6.8$; 12 August, $M7.2$; 21 October, $M6.3$) that almost completely destroyed structures on Kefalonia Island.

The 2003 Lefkada sequence was the key event for the installation of a local network that provided for the first time the proper data for a detailed investigation of the activated main rupture (Karakostas *et al*. 2004), and the activation of secondary structures, which are capable to produce moderate to major earthquakes, thus necessarily to be taken into account in the seismic hazard assessment (Karakostas 2008, Karakostas and Papadimitriou 2010). Accurate microseismicity locations, derived from the recordings of a local network installed and operated on the two Islands (Kefalonia and Lefkada) in 2007-2008, clearly agree with the historical seismicity distribution and extent along the western coasts of both Islands, being located, however, closer to coastlines or onshore (Karakostas *et al*. 2010). Seismicity relocation performed for the purpose of the current study, further confirms this activity location. It is worth to note that during the last period (2007-2014, epicenters shown in red in Fig. 2) the area hosting the 2014 sequence was free of epicenters.

The current seismic excitation is the result of right lateral shear strain accumulated on a zone of weakness, which abuts and slightly overlaps the rupture area of the 1983 main shock ($M7.0$). Both 2014 main shocks and the activated area in general, are located inside stress enhanced areas revealed by the application of the stress evolutionary model (Papadimitriou 2002). The spatio-temporal properties of the sequence, giving more insight to the seismotectonics of this part of the active boundary, reveal the activation of three separate fault segments: the two dextral fault segments almost north-south striking and steeply east-dipping being associated with the two main shocks, along with the ENE-WSW striking also dextral lineaments that form a step-over transfer zone.

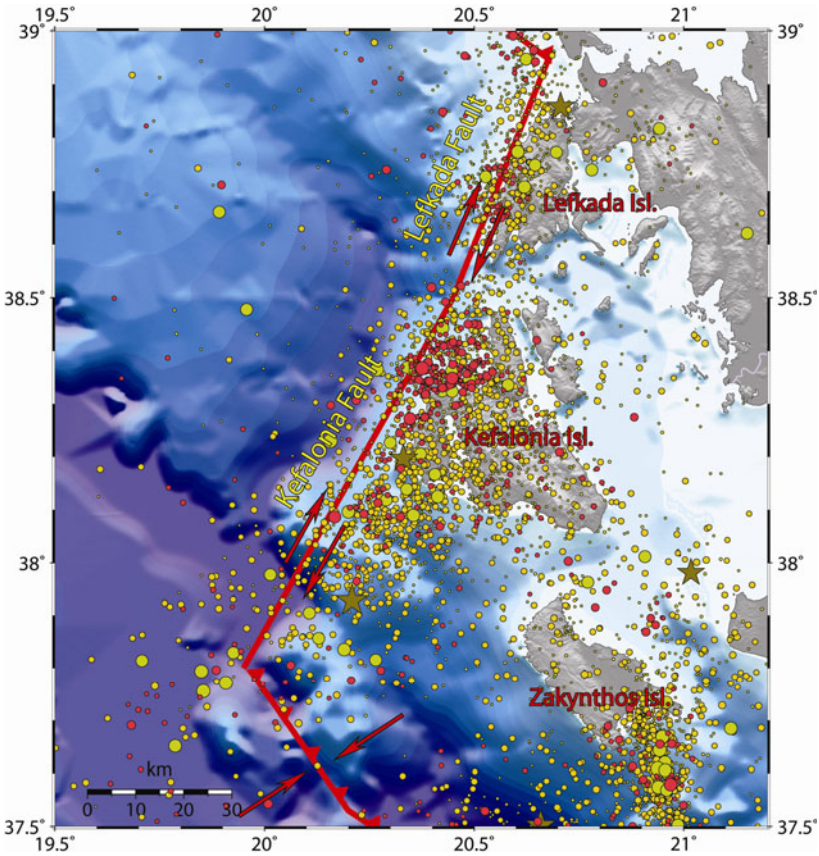

Fig. 2. Relocated seismicity for the period 1983-2013, along with the major active boundaries, the subduction front in the south, the Kefalonia Transform Fault Zone, with the distinctive Kefalonia and Lefkada branches, and the collision boundary north of Lefkada Island. Earthquakes of $M \geq 6.0$, 5.0, 4.0, and 3.0, are depicted by stars, circles, diamonds and squares, respectively, with light grey for the period 1983-2006 and red for 2007 – January 2014.

2. RELOCATION – MAIN SHOCKS AND AFTERSHOCKS SOURCE PARAMETERS

The earthquakes of the 2014 Kefalonia seismic sequence were located using waveform data from stations of the Hellenic Unified Seismological Network (HUSN) and accelerometers operated in the epicentral area by the Institute of Engineering Seismology and Earthquake Engineering (Fig. 3), whereas seismograms readings were carried out by the staff of the Geophysics Department of the Aristotle University of Thessaloniki. The *P*-waves velocity model (Haslinger *et al*. 1999) was used for this purpose (Table 1) – Wadati

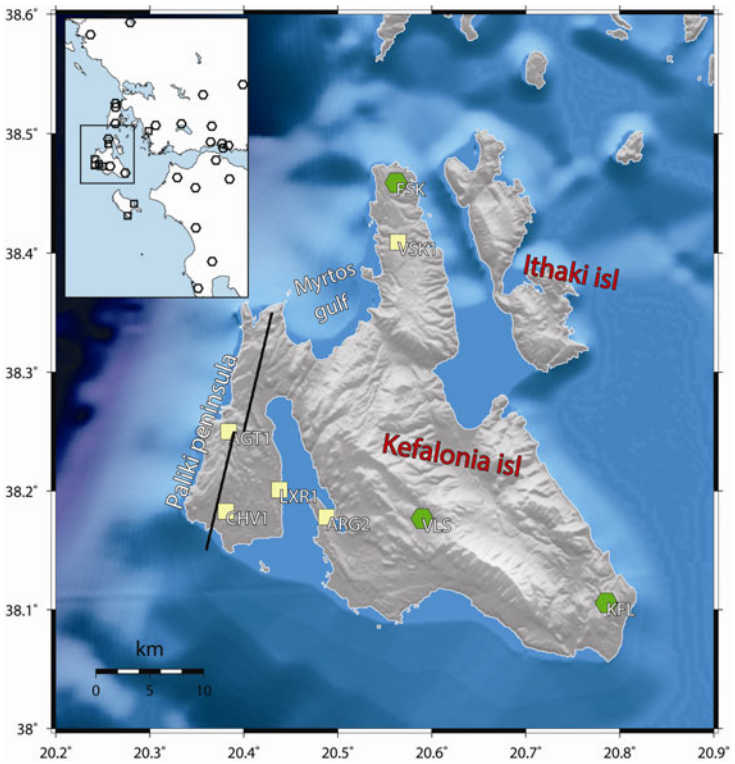

Fig. 3. Locations of the seismological stations (green polygons) of the Unified Hellenic Seismological Network and accelerometers (yellow squares) of the Institute of Engineering Seismology and Earthquake Engineering, installed and operating on Kefalonia Island, and used for aftershock relocation, near the activated fault segments which are shown by black line. The inset map shows the additional stations of the regional seismological network, recordings of which are also used.

Table 1

P-wave velocity model by Haslinger *et al*. (1999) used for the earthquake relocation

Velocity [km/s]	Width [km]
5.47	2.0
5.50	3.0
6.00	5.0
6.20	5.0
6.48	5.0
6.70	10.0
6.75	10.0
8.00	half space

plots based on the recordings of the first days show a *P*- to *S*-wave velocity ratio of $v_p/v_s = 1.78$. Thirty-three seismological stations in epicentral distances less than 150 km were employed for the earthquake location, performed with the HYPOINVERSE computer program (Klein 2000). The azimuthal coverage and the density of the seismological network is satisfactory, controlling adequately the calculated epicenters and focal depths. Several of the stations are inside or very close to the epicentral area, ensuring significantly accurate locations. Time corrections were calculated for all seismological stations, following a procedure of successive iterations until the changes in the calculated time corrections become negligible. In this way lateral variations, which are not included in the 1D velocity model, are taken into account (Karakostas *et al*. 2012, 2014). The data obtained were relocated using the double difference technique (Waldhauser and Ellsworth 2000, Waldhauser 2001). From 1180 earthquakes analyzed until 16 February 2014, 1150 (97%) were relocated, using the catalog data for both *P*- and *S*-phases applying the conjugate gradients method (LSQR, Paige and Saunders 1982). Results were obtained performing 25 iterations by applying distance and misfit weighting after the fifth and tenth iterations, respectively.

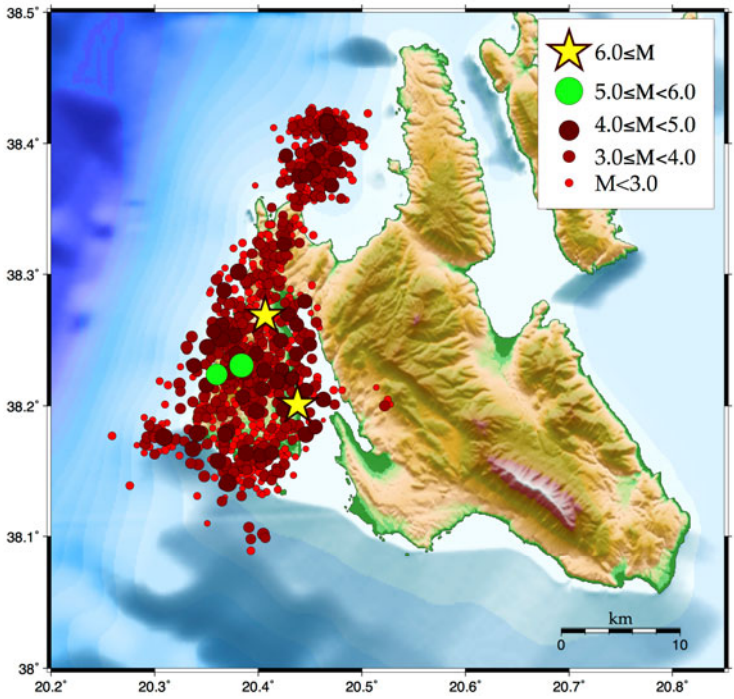

Fig. 4. Relocated aftershock activity of the first 22 days of the sequence (26 January – 16 February 2014).

The aftershock distribution (Fig. 4) for a 22-day period (26 January – 16 February 2014, 1180 earthquakes) reveals a seismic zone trending almost NNE-SSW, parallel to the main axis of the Paliki peninsula, as well as to the north offshore area in Myrtos gulf. The two main earthquakes of the sequence (M_w 6.1 and M_w 6.0, shown as stars) occurred in the southern and the central part of the peninsula, respectively. The seismic sequence started at the southern part of Paliki with the first strong earthquake (M_w 6.1, GCMT solution: strike = 20°/dip = 65°/rake = 177°). In the first 24 hours aftershock activity, particularly earthquakes with $M > 4.0$, is concentrated on an area of about 13 km long, starting from the southern coasts of Paliki and going to the north (Fig. 5a). Further north of this area, up to the northern coasts of the peninsula, seismicity is comparatively low with a lack of $M > 4.0$ events (inside the ellipse of Fig. 5a). In the southernmost part of the low activity area the second main earthquake occurred on 3 February 2014 (Fig. 5b). The aftershocks in the first 24 hours after the second strong event (encompassing

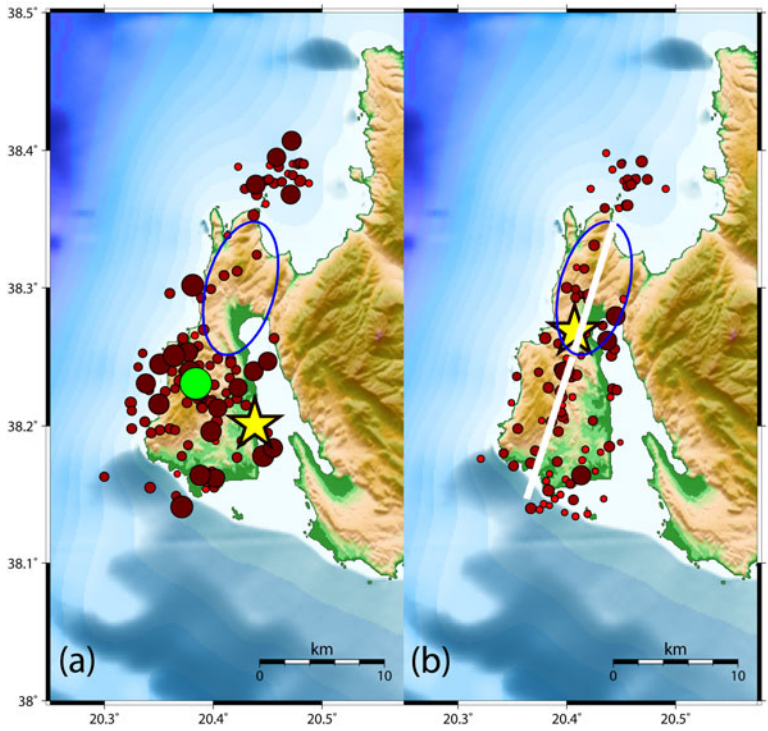

Fig. 5: (a) Aftershock activity for one day after the occurrence of the 26 January 2014 main shock, and (b) one day after the 3 February 2014 main shock. Symbols are the same as in Fig. 4. The ellipse indicates a comparatively low activity area.

in the ellipse in Fig. 5b) are less in number and of smaller magnitudes, in comparison with the first 24 hours activity following the first main shock. However, the seismic zone maintains its dimensions as in the first day of activity, which along with the GCMT focal mechanism (strike = 12°/dip = 45°/rake = 154°) indicate a 10 km-long rupture just north of the first one.

The low activity observed in the rupture area of the second main event soon after the initiation of the sequence, persisted even after the occurrence of the second main shock, implying an asperity that remained locked after the first main shock and that was broken completely during the second main shock. Low seismicity provides evidence for the lack of other smaller faults in this area. The high seismicity in the southern zone, the area associated with the first rupture and the strong aftershock of M5.5 (occurred on 26 January at 18:45, GCMT solution: strike = 11°/dip = 45°/rake = 120°), could be explained as a result of the main rupture, the existence of smaller faults in the area and the stress transfer after the second strong earthquake. Seismicity in the northernmost (offshore) part of the zone is continuous since the beginning of the sequence, which could be considered as a consequence of triggering of smaller faults in this area.

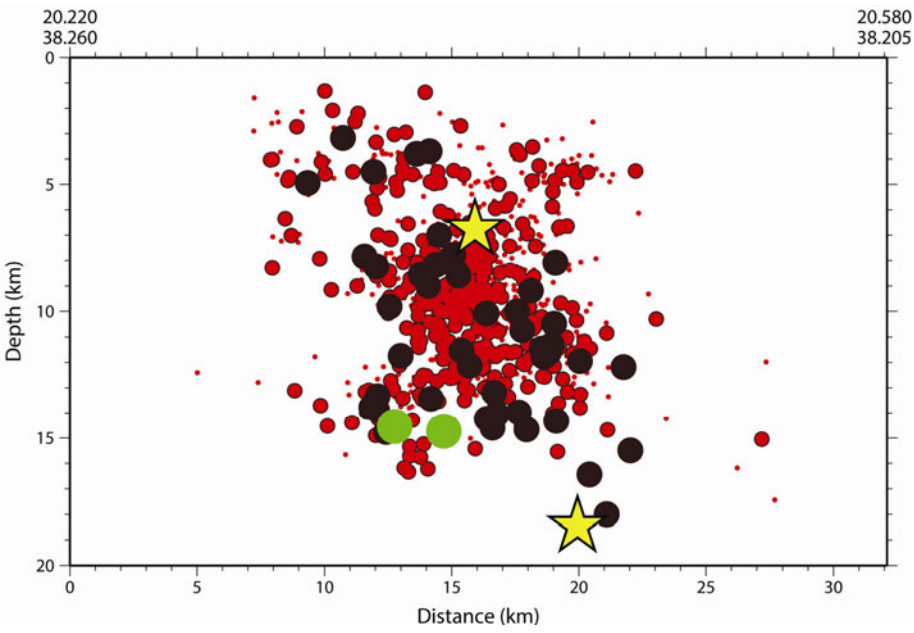

Fig. 6. Cross section normal to the orientation of the aftershock activity. The symbols size is proportional to the earthquake magnitudes. The three larger symbols correspond to earthquakes in the magnitude ranges of 4.0-4.9, 5.0-5.9, and 6.0-6.1.

Figure 6 shows a strike normal cross-section encompassing the aftershocks of both main events. Earthquakes that occurred offshore to the north are not included, since according to our interpretation they are associated with other smaller faults with orientations different than that of the main structure associated with the two main earthquakes. The aftershock zone extends in the range of 2-18 km, dips sharply to the ESE, with the first main shock focus at its lower part. The second main shock occurred at a depth of 7 km, which is probably the reason for the very high values of recorded accelerations. In addition to the main structure, which is delineated clearly from the space distribution of the aftershocks with $M \geq 4.0$, in the cross section the activation of other smaller faults is revealed by the space distribution of the lower magnitude earthquakes as a consequence of the stress transfer due to the coseismic slips of the main shocks. Although it is not completely clear, the strong $M5.5$ aftershock probably occurred on a patch of the main rupture being located between 13-16 km, perhaps in the transition ductile part of the seismogenic layer.

3. FAULT MODEL

Strike-slip faults are commonly segmented at all scales, typically in the form of *en échelon*, non-coplanar faults separated by offsets (or step overs). In our case the step-over zone accommodates continued strike slip displacement between the Kefalonia Fault to the south, and the Lefkada Fault to the north (Fig. 7). This zone comprises smaller parallel fault segments, WSW-ENE striking, almost perpendicular to the *T*-axis orientation at this site, thus controlling the extensional deformation. This set of the closely-spaced parallel seismic lineaments is considered to define strike-slip duplexes and forms a typical transfer zone, between the major Kefalonia and Lefkada Fault segments (shown in Fig. 2), with stepped strike-slip faults and bending in the orientation of the Kefalonia and Lefkada Faults.

In addition to the manifestation of the transfer zone which sheds light on the deformation pattern in the study area, one important component for seismic hazard assessment in particular, is that rupture terminates at this locus, and does not continue further northward. This is repeatedly documented by historical accounts (Papazachos and Papazachou 2003) evidencing that strong earthquakes are associated either with Lefkada or Kefalonia Fault branches separately. The activation of the two branches appeared to be synchronized several times in the past as a result of stress transfer between them (Papadimitriou 2002). One can then assume that the rupture extent has an upper limit that is controlled by the presence of this structure forming bends and stepped strike slip secondary faults, where the orientation of the main fault is deflected.

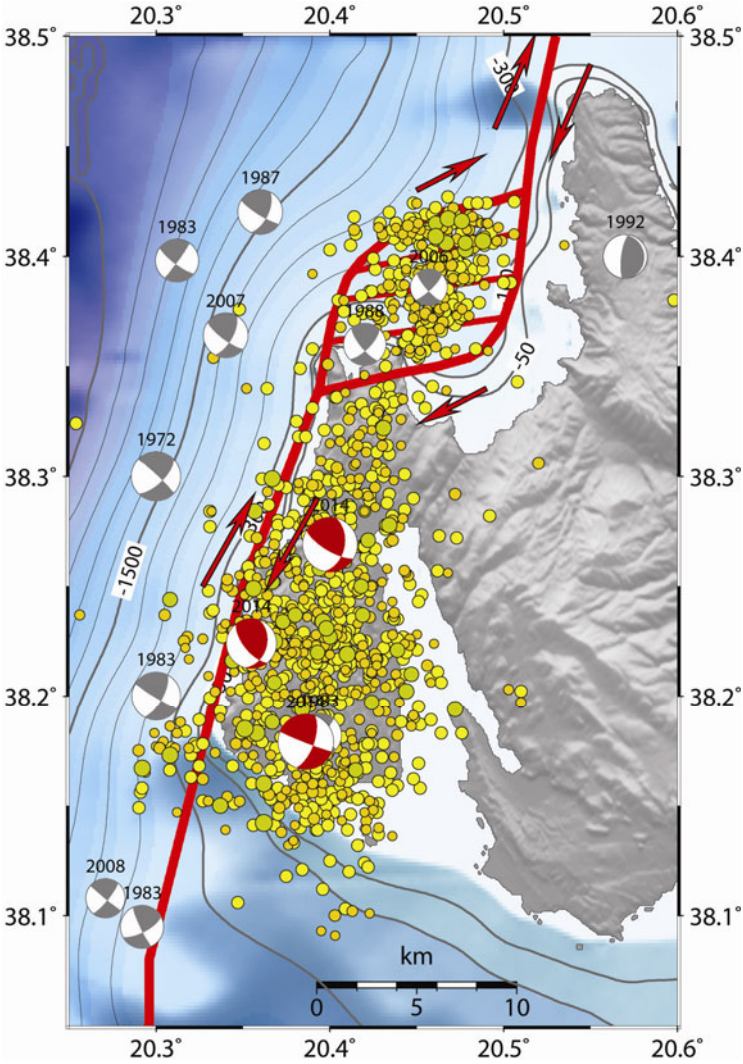

Fig. 7. Aftershock activity (circles) along with inferred fault traces and strong earthquakes fault plane solutions shown as equal area lower hemisphere projections. The compressions quadrants of the stronger earthquakes of the sequence are shown in red. The off fault aftershock activity forms a transfer zone of extensional step overs that connect the Kefalonia Transform Fault to the south with the Lefkada Transform Fault to the north.

4. COULOMB STRESS TRIGGERING

The Coulomb stress change patterns resulting from the two main shocks are shown in Fig. 8. The change in Coulomb failure function (ΔCFF) depends on

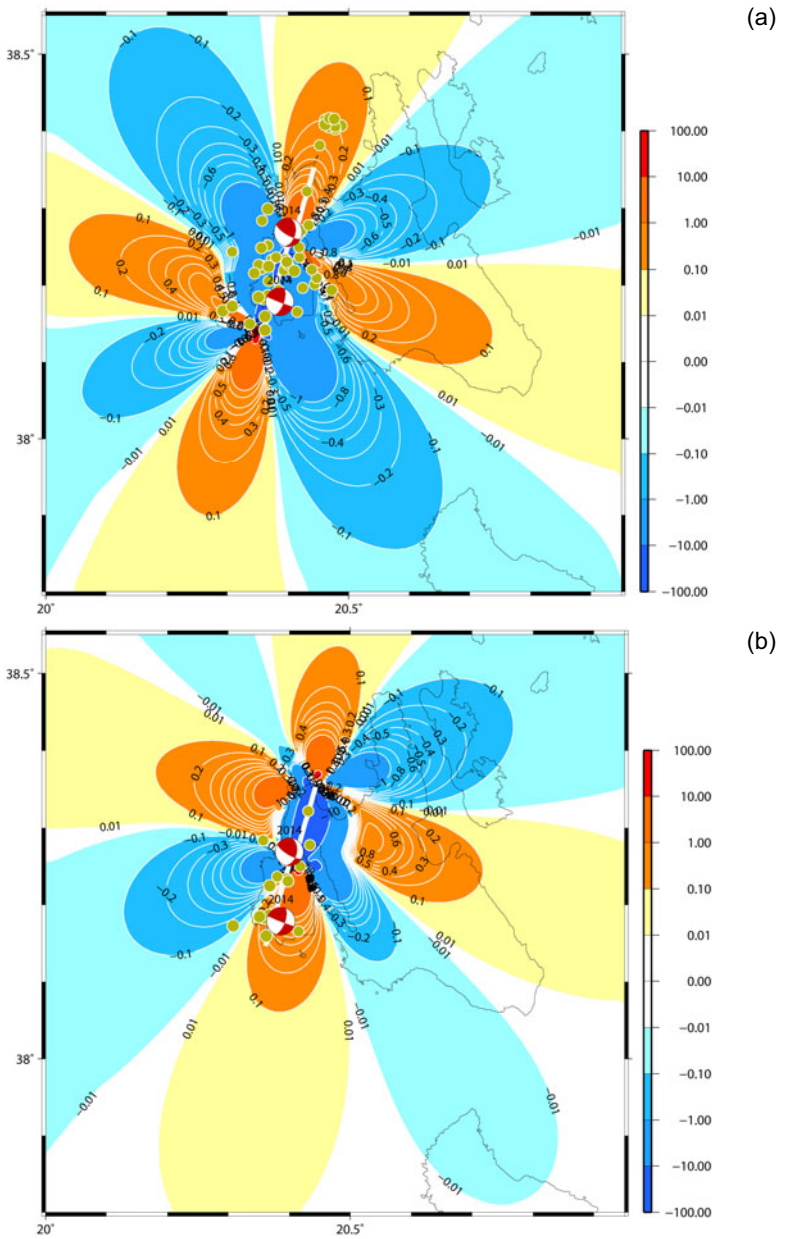

Fig. 8. Coulomb stress changes due to the coseismic slip of: (a) 26 January, and (b) 3 February main shocks, calculated at a depth of 9.0 km. Changes are denoted by the color scale to the right (in bars) and by numbers on the contour lines. The main shock epicenter is depicted by the star and aftershocks by circles, the color and size of which is scaled according to magnitude. The inferred fault trace is shown by the thick white line.

both changes in shear stress, $\Delta\tau$, and normal stress, $\Delta\sigma$, and takes the form $\Delta CFF = \Delta\tau + \mu(\Delta\sigma + \Delta p)$, where Δp is the pore pressure change within the fault, and μ is the friction coefficient which for dry model ranges between 0.6 and 0.8 (Harris 1998 and references therein). Throughout this study we ignore the time-dependent changes in pore fluid pressure and consider only the undrained case (Beeler *et al*. 2000), meaning that Δp depends on the fault-normal stress whereas the fluid mass content per unit volume remains constant. Induced changes in pore pressure resulting from a change in stress under undrained conditions, according to Rice and Cleary (1976) are calculated from $\Delta p = -B(\Delta\sigma_{kk}/3)$, where B is the Skempton's coefficient ($0 \le B \le 1$) and $\Delta\sigma_{kk}$ indicates the summation over the diagonal elements of the stress tensor. We consider a $\mu = 0.75$ and $B = 0.5$, which are close to the case of taking an apparent coefficient of friction $\mu' = 0.4$ suggested by Papadimitriou (2002) who tested different values of μ' for the study area. The shear modulus and Poisson's ratio are fixed as 3.3×10^5 bars and 0.25, respectively. The fault dimensions were defined according to the epicentral distribution and GCMT solutions, as mentioned in a previous section. The centroid moment tensor solutions were adopted for both the faulting type and the value of seismic moment (http://www.ldeo.columbia.edu/~gcmt/). The coseismic slip was then calculated from seismic moment and fault area for both events and the calculations were performed at a depth of 9 km.

Figure 8a evidences high positive stress changes at the location of the northern fault segment, which probably was enhanced and triggered to failure seven days later. The second main event epicenter in particular is located at the southernmost edge of the activated segment, where stress changes have attained the highest positive values (more than 10 bars). The north positive lobe also encompasses the cluster associated with the step over transfer zone. Figure 8b shows that ΔCFF continues to increase at the offshore area; nevertheless, paucity in $M4$ events is observed. Such aftershocks are enhanced in the southern zone instead.

5. DISCUSSION AND CONCLUSIONS

The 2014 Kefalonia doublet (M_w 6.1 and M_w 6.0) with the two main events being separated by seven days in time and about 10 km in space was accommodated by the area comprising Paliki Peninsula and continued offshore northwards, extended over 30-35 km. The rich aftershock production and the spatiotemporal occurrence pattern shed light on the kinematic and structural properties of the activated portions of the KTFZ. The two activated fault segments are compatible with dextral shearing along the Kefalonia Fault branch, the southern portion of which last failed in 1983. The 2014 seismic sequence may be then considered as the spatial continuation of the 1983 sequence with partial coincidence. The aftershock distribution, which ex-

panded up to the northernmost part of the activated area in one day, exhibits a comparatively less active patch, where the second main rupture was accommodated. The aftershock area can be divided into three rupture zones. The southern zone, extending from the first main shock epicenter, covers the southern half of the almost N-S elongated Paliki Peninsula. The second rupture zone starts just north to the first one, evidencing along strike stepping fault segments. To the north of the second zone limit at the northern coast of Paliki and offshore further northwards, a dense cluster appeared almost contemporaneously with the first main shock occurrence. The cluster comprises several $M \geq 4.0$ earthquakes with their number dramatically decreasing after the second main shock occurrence, and can be decomposed in a branch of WSW-ENE striking parallel lineaments.

Both main shocks express north-south dextral strike slip motion, whereas the northern cluster comprises WSW-ENE trending parallel lineaments also of oblique strike-slip motion, dextral with normal component. This constitutes one of the main findings of the current analysis, providing evidence of a transfer zone linking the Kefalonia Fault branch with the Lefkada dextral strike-slip fault branch, which constitutes the northward continuation of Kefalonia Transform Fault Zone.

We used the GCMT focal mechanism solutions and aftershock relocations to construct the source models for calculating the static stress changes due to the two main shocks' coseismic slips. Each earthquake alters the state of stress in its surroundings, and it is advantageous for seismotectonic and seismic hazard recognition purposes to discuss the issue in association with the seismicity manifestation. The offshore cluster triggered by the first main shock occurred in an area where the positive Coulomb stress changes were found to be greater than 0.2 bars, and presented an intense activity encompassing tens of the located aftershocks, several of them having $M \geq 4.0$. This intense activity lasted for about five days and decreased dramatically after the second main shock occurrence, although positive stress changes are accumulated to the ones created by the first main shock. This provides first evidence that the potential of this relay zone cannot exceed moderate magnitude earthquake occurrence. The short duration of the occurrence of stronger aftershocks, might also be the characteristics of the relay zone. The area of Myrtos gulf is characterized by a large number of small magnitude earthquakes in the aftershock period as well as in the last 40 years seismicity (Fig. 2). The area exhibits high activity after the earthquake of magnitude $M5.7$ in 2007. This behavior of seismicity and the absence of any known strong earthquake in the area is an evidence of aseismic movement in the area, which should be investigated using more data. The small magnitude earthquakes are a consequence of rupture of minor geometric anomalies on small faults having different orientations than the main tectonic line. Most

importantly, the later observations set the boundary of the northern extent for the ruptures being originated along the Kefalonia branch of the KTFZ. It also constitutes a major issue for the area's seismic hazard assessment, since it truncates the upper bound of maximum expected earthquake, which is not anticipated to be associated with a rupture exceeding this site to the north.

Acknowledgements. The constructive comments of Sebastiano d'Amico and a second anonymous reviewer, which improved the final version of the paper, are greatly appreciated. Gratitude is also extended to Prof. Telesca for his editorial assistance. Fault plane solutions data used in this paper came from http://www.ldeo.columbia. edu/~gcmt/ and published sources listed in the references. The stress tensors were calculated using a program written by J. Deng (Deng and Sykes 1997), based on the DIS3D code of S. Dunbar, which was later improved (Erikson 1986) and the expressions of G. Converse. The plots were made using the Generic Mapping Tools version 4.5.3 (www.soest.hawaii.edu/gmt, Wessel and Smith 1998). Geophysics Department Contribution 823.

References

Beeler, N.M., R.W. Simpson, S.H. Hickman, and D.A. Lockner (2000), Pore fluid pressure, apparent friction, and Coulomb failure, *J. Geophys. Res*. **105**, B11, 25533-25542, DOI: 10.1029/2000JB900119.

Deng, J., and L.R. Sykes (1997), Evolution of the stress field in southern California and triggering of moderate-size earthquakes: A 200-year perspective, *J. Geophys. Res*. **102**, B5, 9859-9886, DOI: 10.1029/96JB03897.

Erickson, L. (1986), User's manual for DIS3D: A three-dimensional dislocation program with applications to faulting in the Earth, M.Sc. Thesis, Geomechanics Applied Earth Science Dept., Stanford University, Stanford, USA, 167 pp.

Harris, R.A. (1998), Introduction to special section: Stress triggers, stress shadows, and implications for seismic hazard, *J. Geophys. Res*. **103**, B10, 24347-24358, DOI: 10.1029/98JB01576.

Haslinger, F., E. Kissling, J. Ansorge, D. Hatzfeld, E. Papadimitriou, V. Karakostas, K. Makropoulos, H.-G. Kahle, and Y. Peter (1999), 3D crustal structure from local earthquake tomography around the gulf of Arta (Ionian region, NW Greece), *Tectonophysics* **304**, 3, 201-218, DOI: 10.1016/S0040-1951(98)00298-4.

Karakostas, V. (2008), Relocation of aftershocks of the 2003 Lefkada sequence: Seismotectonic implications. **In:** *Proc. 3rd Hellenic Conf. Earthquake En-*

gineering and Engineering Seismology, 5-7 November 2008, *Athens, Greece*, CD ROM, 16 pp.

Karakostas, V.G., and E.E. Papadimitriou (2010), Fault complexity associated with the 14 August 2003 M_w6.2, Lefkada, Greece, aftershock sequence, *Acta Geophys.* **58**, 5, 838-854, DOI: 10.2478/s11600-010-0009-6.

Karakostas, V.G., E.E. Papadimitriou, and C.B. Papazachos (2004), Properties of the 2003 Lefkada, Ionian Islands, Greece, earthquake seismic sequence and seismicity triggering, *Bull. Seismol. Soc. Am.* **94**, 5, 1976-1981, DOI: 10.1785/012003254.

Karakostas, V.G., E.E. Papadimitriou, Ch.K. Karamanos, and D.A. Kementzetzidou (2010), Microseismicity and seismotectonic properties of the Lefkada–Kefalonia seismic zone, *Bull. Geol. Soc. Greece* **43**, 2053-2063.

Karakostas, V., E. Karagianni, and P. Paradisopoulou (2012), Space-time analysis, faulting and triggering of the 2010 earthquake doublet in western Corinth Gulf, *Nat. Hazards* **63**, 2, 1181-1202, DOI: 10.1007/s11069-012-0219-0.

Karakostas, V., E. Papadimitriou, and D. Gospodinov (2014), Modelling the 2013 North Aegean (Greece) seismic sequence: geometrical and frictional constraints, and aftershock probabilities, *Geophys. J. Int.* **197**, 1, 525-541, DOI: 10.1093/gji/ggt523.

Kiratzi, A.A., and C.A. Langston (1991), Moment tensor inversion of the 1983 January 17, Kefallinia event of Ionian islands (Greece), *Geophys. J. Int.* **105**, 2, 529-535, DOI: 10.1111/j.1365-246X.1991.tb06731.x.

Klein, F.W. (2000), User's guide to HYPOINVERSE-2000, a Fortran program to solve earthquake locations and magnitudes, Open File Rep. 02-171, Ver. 1.0, U.S. Geological Survey, Menlo Park, USA.

Kokinou, E., E. Papadimitriou, V. Karakostas, E. Kamberis, and F. Vallianatos (2006), The Kefalonia Transform Zone (offshore Western Greece) with special emphasis to its prolongation towards the Ionian Abyssal Plain, *Mar. Geophys. Res.* **27**, 4, 241-252, DOI: 10.1007/s11001-006-9005-2.

Louvari, E., A.A. Kiratzi, and B.C. Papazachos (1999), The Cephalonia Transform Fault and its extension to western Lefkada Island (Greece), *Tectonophysics* **308**, 1-2, 223-236, DOI: 10.1016/S0040-1951(99)00078-5.

Paige, C.C., and M.A. Saunders (1982), Algorithm 583: LSQR – sparse linear equations and least squares problems, *ACM Trans. Math. Software* **8**, 2, 195-209, DOI: 10.1145/355993.356000.

Papadimitriou, E.E. (1993), Focal mechanism along the convex side of the Hellenic Arc, *Boll. Geof. Teor. Appl.* **35**, 140, 401-426.

Papadimitriou, E.E. (2002), Mode of strong earthquake recurrence in the central Ionian Islands (Greece): Possible triggering due to Coulomb stress changes generated by the occurrence of previous strong shocks, *Bull. Seismol. Soc. Am.* **92**, 8, 3293-3308, DOI: 10.1785/0120000290.

Papadimitriou, E.E., and B.C. Papazachos (1985), Evidence for precursory seismicity patterns in the Ionian Islands (Greece), *Earthq. Predict. Res.* **3**, 95-103.

Papazachos, B.C., and C.C. Papazachou (2003), *The Earthquakes of Greece*, Ziti Publ., Thessaloniki, 304 pp.

Rice, J.R., and M.P. Cleary (1976), Some basic stress diffusion solutions for fluid-saturated elastic porous media with compressible constituents, *Rev. Geophys*. **14**, 2, 227-241, DOI: 10.1029/RG014i002p00227.

Scordilis, E.M., G.F. Karakaisis, B.G. Karakostas, D.G. Panagiotopoulos, P.E. Comninakis, and B.C. Papazachos (1985), Evidence for transform faulting in the Ionian Sea: The Cephalonia Island earthquake sequence of 1983, *Pure Appl. Geophys.* **123**, 3, 388-397, DOI: 10.1007/BF00880738.

Waldhauser, F. (2001), HypoDD – A program to compute double-difference hypocenter locations, Open File Rep. 01-113, U.S. Geological Survey, Menlo Park, USA.

Waldhauser, F., and W.L. Ellsworth (2000), A double-difference earthquake location algorithm: Method and application to the Northern Hayward Fault, California, *Bull. Seismol. Soc. Am*. **90**, 6, 1353-1368, DOI: 10.1785/0120000006.

Wessel, P., and W.H.F. Smith (1998), New, improved version of Generic Mapping Tools released, *EOS Trans. Am. Geophys. Union* **79**, 47, 579, DOI: 10.1029/98EO00426.

Received 8 April 2014
Received in revised form 9 June 2014
Accepted 9 June 2014